

Estimation of LINAC X-ray Fluence Rate in a High-Energy Region Using Activation Detectors

Kazuo KATO Yuko MOTIZUKI
Toshinori MASUMOTO Tadashi KOYAMA

Department of Radiological Sciences, Faculty of Health and Welfare,
Hiroshima Prefectural College of Health Sciences

Received 12 September 2006

Accepted 12 December 2006

Abstract

Fluence rate of 10 MV X-rays from the electron linear accelerator (LINAC) for radiation therapy at the Prefectural University of Hiroshima was estimated by measuring gamma rays from activities induced by X-rays in zinc, copper and indium metals. The gamma-ray measurements were performed using a large volume (160 cm³) Ge detector. The X-ray exposure was conducted so that the absorbed dose rate at a 5cm depth for radiation therapy was 2 Gy/min. The measurements showed that ⁶³Zn, ⁶²Cu and ^{115m}In activities were induced in those metals. The estimated fluence rates were $(1.43 \pm 0.15) \times 10^{13} \text{ m}^{-2} \text{ s}^{-1}$ in 5-10 MeV, $(3.15 \pm 0.20) \times 10^{11} \text{ m}^{-2} \text{ s}^{-1}$ in 10-12 MeV and $(1.51 \pm 0.16) \times 10^{10} \text{ m}^{-2} \text{ s}^{-1}$ in 12-15 MeV, at the isocenter 20 cm above the couch. The uncertainties of fluence rates do not include those due to the uncertainties of the cross sections. The fluence rates were estimated assuming that the fluence rate of the X-rays of energy larger than 15 MeV was negligible. The X-rays in the energy region higher than 10 MeV scarcely contributed to the X-ray doses for radiation therapy. However, X-rays of such high energies can induce many kinds of photonuclear reactions in the materials used in the LINAC. In our previous study, relatively large thermal neutron fluence was observed in the exposure room. The X-rays in the energy region beyond 10 MeV presumably cause a large part of the photoneutron productions.

Key words : LINAC, photonuclear reaction, radiation therapy, X-ray

Introduction

Some of linear electron accelerators (LINACs) for medical use were operated with electron energy of 15 MeV or the more. Although X-rays produced by such high energy electrons are convenient for treatment of malignant tumors at deep positions, intensities of unfavorable photon neutrons are very high. The LINAC for medical use in Prefectural University of Hiroshima (Mitsubishi, EXL-15DP) is usually operated with 10 MeV acceleration energy. Kato, *et al.*¹⁾ showed that the thermal neutron fluence under the head was so large that an Indium (In) foil was useful to measure the fluences even at deep positions in a stack of polyethylene plates. A few photonuclear reactions in the materials used in LINAC are induced by photons of energies less than 10 MeV. Large thermal neutron fluence rates observed in our previous research suggest that X-rays of energies close to 10 MeV is not negligible. Therefore, in order to control the photon neutrons caused by LINAC X-rays, experimental estimation of X-ray energy distribution is necessary.

Tissue-maximum dose Ratio (TMR) weakly relates to the detail of X-ray energy distribution around 10 MeV, because the dose from X-rays of energies near primary electron beam energy is much smaller than those from the X-rays in the lower energy region. Ordinary detectors to photon such as semiconductor detector are sensitive for low energy photons. Therefore, ordinary detectors are also inappropriate for examining the X-ray energy distribution around 10 MeV. In our previous measurements of gamma rays from In activation foils exposed to 10 MV X-rays, the gamma ray from ^{115m}In was also detected¹⁾. This activity can be induced by high energy X-rays. A set of such activation detectors is available for estimating X-ray energy distributions around 10 MeV without disturbance by low energy X-rays.

Materials and Methods

In the LINAC used in this study, the target, collimator and flattening filter were made of copper (Cu), lead and stainless steel, respectively. When 6 MV X-rays were produced, the target is replaced by a platinum one. The activation detectors were zinc (Zn), Cu, indium and potassium chloride (KCl). The reactions expected in the detectors are also shown in Table 1. The detector samples were exposed to X-rays on an aluminum sheet of 15 μ m in thickness, 20 cm above the couch. The field size was 10 cm \times 10 cm, and the X-rays output rate corresponded to the dose rate of 2 Gy/min at 5 cm depth for radiation therapy. The exposure time was one minute for indium, and five minutes for the other elements. Indium grains (Wako Chemical Co., Ltd),

0.190 g were used to make an In foil of 0.5 cm in radius. A circular Zn foil, 9.65 g of mass and 2.3 cm in radius was cut out from a purchased Zn plate (Shimadzu Rika Co., Ltd). A circular Cu foil of 18.7 g in mass and 2.1 cm in radius was also cut out from a purchased Cu plate (Shimadzu Rika Co., Ltd). A polyethylene envelope of 20 μ m in thickness was used to contain 9.98 g of KCl powder (Wako Chemical Co., Ltd). The area of the powder was 20.25 cm².

The samples exposed to X-rays were mounted on the window of a Ge-semiconductor detector (OXFORD CPVDS30-0190) in a lead shield which was thicker than 15 cm. Detection efficiencies were determined using two circular ¹⁵²Eu calibration sources with diameters were 1.4 cm and 3.6 cm. The circular calibration sources were made from the standard solution (Japan Isotope Cooperation, EU050) of which specific activity was guaranteed within 2.3 % of uncertainty. One ml of standard solution was used to make each circular source. The mass of the solution was measured with 0.3 % uncertainty using an electric balance. The smaller circular calibration source was used for estimating the detection efficiency of the gamma rays from indium-plate, and the larger one was used for those for the other metal foils. The estimated efficiency was modified for a small change of the detection efficiency due to the difference between the radius of sample and that of the calibration source. The correction factor was estimated from the detection efficiencies of 344 keV gamma ray from a point-like ¹⁵²Eu standard source (Japan Isotope Cooperation, EU-402) at various positions on the window of the Ge detector. The ¹⁵²Eu calibration source allowed us to determine the detection efficiencies in the energy region lower than 1.4 MeV. The gamma ray from ³⁸K is higher than 1.4 MeV, and the detection efficiency has not been determined. The specific activities immediately after exposure were determined analyzing the full energy peaks in the measured spectra for the three metal foils mentioned above. The X-ray fluences were calculated from the specific activities and the cross-sections of photonuclear reactions. The thresholds of the reactions were calculated by the data of nuclear mass²⁾. The cross sections of photonuclear reactions were quoted from the EXFOR database and Japanese Evaluated Nuclear Data Library^{3,4)}. The energy region from 5 MeV to 15 MeV was divided into three small regions, and the mean cross sections were calculated assuming that the photon energy distribution in each small region was constant except in the region of 5-10 MeV. The mean cross section of ¹¹⁵In(X, X') ^{115m}In in this energy region was calculated assuming that the energy differential fluence rate of 10 MV X-rays was in proportion to difference between the photon energy and 10 MeV. In this study, we assumed that few X-rays of energies

greater than 15 MeV were emitted. The cross section for $^{115}\text{In}(X,X')^{115\text{m}}\text{In}$ for X-ray of energy larger than 12 MeV was estimated by extrapolation using the cross section from 11 MeV to 12 MeV, and the cross section was assumed to be zero beyond 13 MeV. Moreover, we assumed no production of $^{115\text{m}}\text{In}$ by X-rays with energies less than 5 MeV. The mean cross sections used in this study are shown in Table 1. The reaction rates of $^{64}\text{Zn}(X,n)^{63}\text{Zn}$, $^{63}\text{Cu}(X,n)^{62}\text{Cu}$ and $^{115}\text{In}(X,X')^{115\text{m}}\text{In}$ were used to estimate the X-ray energy fluence rates in the three energy regions. We have found no data on the cross sections of $^{39}\text{K}(X,n)^{38\text{g}}\text{K}$ (7.636 min). The photonuclear reactions in KCl induce not only $^{38\text{g}}\text{K}$ but also $^{38\text{m}}\text{K}$ (0.925 s), and the $^{38\text{m}}\text{K}$ nucleus directly decays into ^{38}Ar . The data on the $^{38\text{g}}\text{K}$ production rate was used for considering whether the LINAC emitted X-rays with energies beyond the threshold energy, 13.1 MeV.

Results

The gamma-ray spectrum measured for Zn foil is shown in Fig.2. The activity of ^{63}Zn in Zn foil is produced only by $^{64}\text{Zn}(X,n)^{63}\text{Zn}$ reaction. The threshold neutron energy for $^{64}\text{Zn}(n,2n)^{63}\text{Zn}$ reaction is 11.9 MeV, and hence the neutrons from the LINAC cannot induce the reaction. The gamma-ray spectrum measured for Cu foil is shown in Fig.3. The ^{62}Cu nuclei in the foil were produced only by $^{63}\text{Cu}(X,n)^{62}\text{Cu}$ reaction. The reaction of $^{63}\text{Cu}(n,2n)^{62}\text{Cu}$ scarcely occurs in the copper material under the LINAC head. Positron is emitted in the decay of ^{62}Cu , and the annihilation gamma rays were observed. In the copper material, the ^{64}Cu activity was also induced by $^{63}\text{Cu}(n,\gamma)^{64}\text{Cu}$ and $^{65}\text{Cu}(X,n)^{64}\text{Cu}$ reactions. The threshold energy of $^{65}\text{Cu}(X,n)^{64}\text{Cu}$ reaction is 9.9 MeV. As shown in Fig.4, gamma-ray measurement was repeated 14 times until about 2 hours after the end of exposure to LINAC X-rays, and the ^{62}Cu activity was calculated from the counts in the annihilation gamma-ray full energy peaks and the half-lives of ^{64}Cu and ^{62}Cu .

The gamma ray spectrum measured for In foil is shown in Fig.5. The spectrum clearly shows that both $^{116\text{m}}\text{In}$ and $^{115\text{m}}\text{In}$ were induced in the In foil. The $^{116\text{m}}\text{In}$ nuclei were produced by thermal neutrons through $^{115}\text{In}(n,\gamma)^{116\text{m}}\text{In}$ reactions. Not only X-ray but also fast neutron can induce $^{115\text{m}}\text{In}$ activity in In foil. In this study, we concluded that the $^{115\text{m}}\text{In}$ activity was induced by the inelastic interaction of X-ray with ^{115}In . The reason is described in the section of discussion.

The gamma ray spectrum measured for KCl is shown in Figure 6. The measurement for five minutes was repeated three times after the exposure to 10 MV X-rays, and the half-life of the parent nuclide for 2167 keV gamma ray was

estimated to be 6.3 ± 1.7 min. This is almost coincident with the half-life of $^{38\text{g}}\text{K}$ of which half-life is 7.74 min. The 2167 keV and 1643 keV gamma rays are emitted in the decay of ^{38}Cl , of which half life is 37.24 min. The intensity of 2167 keV gamma ray is 42.4%, and that of 1643 keV gamma ray is 31.9%²⁾. As shown in Fig.6, there was no counts at the channels for 1643 keV full energy peak. Thus, we concluded that the 2167 keV gamma-ray counts were given by the decays of $^{38\text{g}}\text{K}$ radioisotopes.

The production rates per one target nucleus were determined analyzing the spectra, and the results are shown in Table 2. Using the mean cross section shown in Table 1, the fluence rates were calculated, as shown in Table 3.

Discussion

The activity of $^{115\text{m}}\text{In}$ in In foil was produced not only by X-ray but also by fast neutrons. Fast neutron fluence under the LINAC head has not been determined. Barquero, *et al.*⁵⁾ calculated the spectrum of the neutrons from 18 MV LINAC. On the patient couch, the fast neutron fluence around 1 MeV was less than that in thermal region⁵⁾. The cross section of $^{115}\text{In}(n,n')^{115\text{m}}\text{In}$ increases from 0.4 MeV until 3 MeV, and approximately 60 mb at 1 MeV³⁾. The thermal neutron fluence rate, roughly $3 \times 10^7 \text{ m}^{-2} \text{ s}^{-1}$ was estimated from the $^{116\text{m}}\text{In}$ production rate obtained in our preliminary study. Assuming that the fast neutron fluence around 1 MeV was same as thermal neutron fluence, the production rate of $^{115\text{m}}\text{In}$ during the exposure was estimated to have been $1.8 \times 10^{-22} \text{ s}^{-1}$ per one ^{115}In nucleus. This rate was much less than that measured in this study. (See Table 2.) The production rates in the other energy regions were probably negligible, because the cross section was very low in the lower energy side and neutron fluence was presumably very low in the higher one. In our previous study, a 3 cm Cu filter between In foil and LINAC head reduced the activity of $^{115\text{m}}\text{In}$. The decrease rate was approximately coincident with that in the X-ray intensity¹⁾. Moreover, 6 MV X-rays also produced $^{115\text{m}}\text{In}$ in the indium foil¹⁾. The 6MV X-rays produced few photoneutrons. Therefore, we concluded that not fast neutron but X-ray induced the $^{115\text{m}}\text{In}$ activity in the indium foil. As mentioned above, the $^{115\text{m}}\text{In}$ activities measured in this study were used to estimate the X-ray fluence rate in the wide energy region, 5-10 MeV. The estimated fluence rate strongly depends on the cross section for the inelastic scattering, which is shown in Fig.1. The more activation detectors will be used for precisely estimating the fluence rate of X-rays of energies lower than 10 MeV in near future.

In our preliminary study, the TMR for 10 MV X-ray was measured using the dosimeter (PTW, Type 23333). The

TMR values at 10 cm, 15 cm, 20 cm and 25 cm depth in tissue-equivalent block (KyotoKagaku, Tough-Water Phantom) were compared with those reported by Jordan⁶⁾. The results showed that the primary original electron beam energy was 10.2 ± 0.6 MeV, which agreed well with the nominal energy, 10 MeV. As shown in Table 3, the present X-ray fluence rate in the energy region beyond 10 MeV was much smaller than that in the energy region from 5 MeV to 10 MeV. Therefore, we consider that the X-rays of energies higher than 10 MeV give little dose influence to patient's body.

X-rays of energies over 10 MeV probably induced many kinds of photonuclear reaction in the materials of the LINAC. For example, threshold energy for (X, n) reaction in ⁵⁶Fe is 11.2 MeV and that in ⁶³Cu is 10.9 MeV. The major element in the flattening filter is ⁵⁶Fe, and that in the target is ⁶³Cu. The main element of collimator is ²⁰⁸Pb. The threshold energy for ²⁰⁸Pb(X, n)²⁰⁷Pb is 7.4 MeV, and the cross section increases as the X-ray energy increases until 13.4 MeV⁴⁾. The natural abundance of ¹⁴N in nitrogen is 99.4%, and the threshold energy for ¹⁴N(X, n)¹³N reaction is 10.6 MeV. Since nitrogen is one of the important elements in human tissue, it is necessary to turn our attention to the photonuclear reactions in ¹⁴N nuclei even when 10 MV X-rays is used.

Chibani and Ma⁷⁾ showed that 15 MV and 18 MV X-rays in a Varian 2160C LINAC produce more neutrons than 18 MV beam in a Siemens Primus LINAC, because their primary electron energies, 15 and 18.3 MeV were higher than 14 MeV for the Siemens 18MV X-rays. This suggests that the primary electron energy is not always fitted to the nominal energy with small uncertainty. Moreover, the present study showed that the LINAC X-rays had energies higher than the maximum energy estimated by the measurement of TMR. The present study revealed that the activation detectors were available for estimating the energy distribution of X-rays in such high-energy region. The X-ray fluence rates determined in this study have uncertainties due to those of photonuclear cross sections. In this study only three reactions were used for estimation of fluence rate. The photonuclear cross sections for many nuclides have been usable^{3,4,8)}. The more accurate estimation of the X-ray fluence rate will be established using the more activation detectors.

Conclusion

Measuring the gamma rays from Zn, In, Cu and KCl exposed to the 10 MV X-rays, we could observe the activities induced by photo-inelastic scattering and photonuclear reaction. Assuming that no X-ray of energy larger than 15 MeV was included in the 10 MV X-rays, the X-ray fluence

rates in the energy range from 5 MeV to 15 MeV were estimated using the data of the activities and the cross sections. In the estimation, the uncertainties of the cross sections were not considered. The estimated fluence rates were $(3.15 \pm 0.20) \times 10^{11} \text{ m}^{-2} \text{ s}^{-1}$ at the 10 - 12 MeV region, $(1.51 \pm 0.16) \times 10^{10} \text{ m}^{-2} \text{ s}^{-1}$ at the 12 - 15 MeV region, and $(1.43 \pm 0.15) \times 10^{13} \text{ m}^{-2} \text{ s}^{-1}$ estimated at the 5-10 MeV region. The fluence rates of the X-rays of energy larger than 10 MeV were not negligible, but were much less than that at the 5-10 MeV region.

Acknowledgement

The authors are grateful to Mr. Shigehisa Tanaka (Sendai Kousei Hospital) for his help in a part of the experiments.

References

- 1) Kato, K., Omi, M., et al. : Mean Energy of Neutrons from an Electron Linear Accelerator for Radiation Therapy. *Journal of Hiroshima Prefectural College of Health Sciences: Humanity and Science* 5: 31-40, 2005
- 2) Firestone, R.B. Chu, S.Y.F. and Baglin, C.M. (editors) : Table of Isotopes CD ROM (Eighth Edition: 1999 Update), Wiley-InterScience, 1999
- 3) EXFOR / CSISRS Experimental Nuclear Reaction Data (Database Version of August 17, 2006) at <http://www.nndc.bnl.gov/exfor3/exfor00.htm>
- 4) Japanese Evaluated Nuclear Data Library, JENDL. Retrieved Sep, 2006, from http://www.wndc.tokai-sc.jaea.go.jp/jendl/Jendl_J.html
- 5) Barquero, R., Mendez, R., et al. : Neutron spectra and dosimetric features around an 18 MV LINAC accelerator. *Health Phys.* 88: 48-58, 2005
- 6) Jordan, T.J.: Megavoltage X-ray beams: 2-50 MV. *British Journal of Radiology*, Suppl.2: 62-109, 1996
- 7) Chibani, C. and Ma, C.M.C. : Photonuclear dose calculations for high-energy photon beams from Siemens and Varian linacs. *Med. Phys.* 30: 1990-2000, 2003
- 8) Storm, V. and Israel, V.: Photon cross-sections from 1 keV to 100 MeV for elements Z=1 to Z=100*. *Nuclear Data Tables*, A7: 565-681, 1970

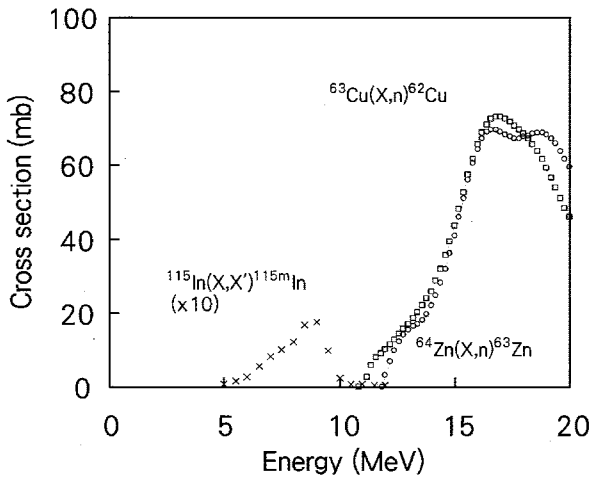


Fig.1 Cross sections of $^{64}\text{Zn}(\text{X},\text{n})^{63}\text{Zn}$ and $^{63}\text{Cu}(\text{X},\text{n})^{62}\text{Cu}$ reactions and $^{115}\text{In}(\text{X},\text{X}')^{115\text{m}}\text{In}$ inelastic scattering^{3,4)}. Ten times cross section for $^{115}\text{In}(\text{X},\text{X}')^{115\text{m}}\text{In}$ is indicated. Squares show the cross section for $^{63}\text{Cu}(\text{X},\text{n})^{62}\text{Cu}$ reaction, and circles show that for $^{64}\text{Zn}(\text{X},\text{n})^{63}\text{Zn}$ one.

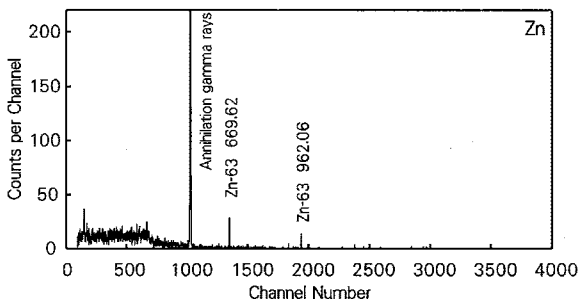


Fig.2 Gamma-ray spectrum for zinc foil. The measurement started 38 min after the end of the X-ray exposure, and lasted for 600 s.

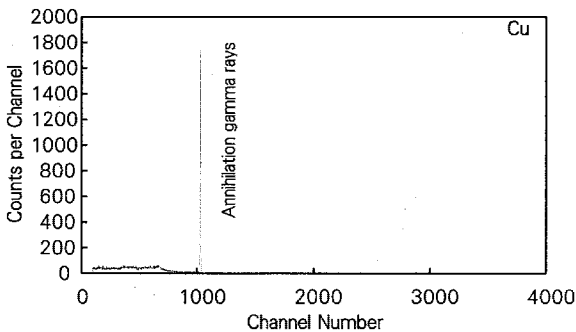


Fig.3 Gamma ray spectrum measured for copper foil. The measurement started 7 min after the end of the X-ray exposure, and lasted for 300 s.

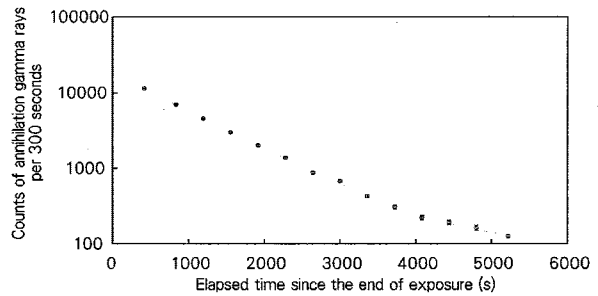


Fig.4 Elapsed time dependence of counts of annihilation gamma rays from copper foil. The annihilation gamma rays were produced by decays of ^{64}Cu (762 min) and ^{62}Cu (9.74 min) in the copper foil exposed to LINAC X-rays and neutrons. The last measurement started 87 min after the end of exposure, and lasted for 1800 s. The peak counts divided by six was shown in the figure. The count rates of annihilation gamma rays from ^{64}Cu and ^{62}Cu immediately after the end of exposure were determined from the peak counts for the annihilation γ rays by method of least squares. The solid line in the figure shows the counts calculated from the determined count rates.

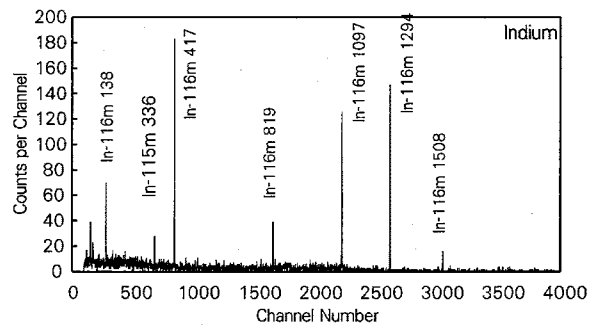


Fig.5 Gamma ray spectrum measured for indium foil. The measurement started 40 min after the end of the X-ray exposure, and lasted for 600 s.

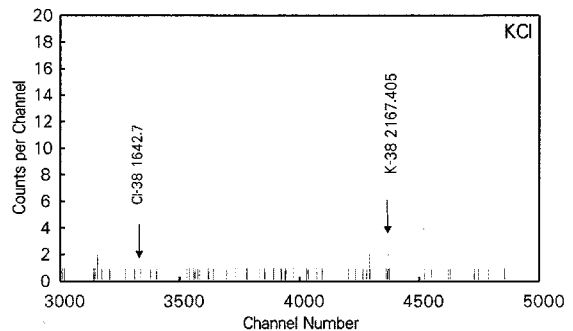


Fig.6 Gamma ray spectrum measured for potassium chloride. The measurement started 5 min after the end of the X-ray exposure, and lasted for 5 min.

Table 1. Threshold energy and the mean cross section of photonuclear reaction in the materials exposed to 10 MV X-rays^{2,3,4)}.

Material	Photonuclear reaction (Half life of induced nuclide)	Threshold energy (MeV)	Mean cross section (mb) in		
			5-10 MeV	10-12 MeV	12-15 MeV
Zn	$^{64}\text{Zn}(\text{X},\text{n})^{63}\text{Zn}$ (38 min)	11.9	0	0	14.801
Cu	$^{63}\text{Cu}(\text{X},\text{n})^{62}\text{Cu}$ (9.74 min)	10.9	0	0.320	19.955
In	$^{115}\text{In}(\text{X},\text{X}')^{115\text{m}}\text{In}$ (4.486 h)	0.336	0.592	0.068	0.007
KCl	$^{39}\text{K}(\text{X},\text{n})^{38}\text{K}$ (7.636 min)	13.1			

Table 2. The production rates of ^{63}Zn , ^{62}Cu and $^{115\text{m}}\text{In}$

Nuclide	Production rate per second per target nucleus (s^{-1})
^{63}Zn	$(3.30 \pm 0.30) \times 10^{-20}$
^{62}Cu	$(1.55 \pm 0.06) \times 10^{-19}$
$^{115\text{m}}\text{In}$	$(8.46 \pm 0.89) \times 10^{-19}$

Table 3. X-ray fluence rate in high energy region

Energy region (MeV)	Fluence rate ($\text{m}^{-2} \text{s}^{-1}$)
5-10	$(1.43 \pm 0.15) \times 10^{13}$
10-12	$(3.15 \pm 0.20) \times 10^{11}$
12-15	$(1.51 \pm 0.16) \times 10^{10}$

ライナック X線の高エネルギー領域における フルエンス率の放射化検出器による推定

加藤 一生 望月 裕子 舛本 俊典 小山 矩

広島県立保健福祉大学保健福祉学部放射線学科

2006年 9月12日受付

2006年 12月12日受理

抄録

県立広島大学で放射線治療に用いられている電子線直線加速器(ライナック)からの10 MV X線のエネルギー分布を, X線を照射した亜鉛, 銅ならびにインジウムに生じた放射能からの γ 線を測定することにより推定した。 γ 線測定は大きなGe半導体検出器(160 cm³)を用いて測定した。X線照射は治療時の深さ5cmにおける吸収線量率が2 Gy/minとなるように行った。測定の結果, 照射金属中に⁶³Zn, ⁶²Cuならびに^{115m}Inがそれぞれ生成されていることが分かった。治療台から20 cm上のアイソセンターにおいて推定したX線フルエンス率はX線のエネルギー 5-10 MeVで $(1.43 \pm 0.15) \times 10^{13}$ (m² s⁻¹), 10-12 MeVで $(3.15 \pm 0.20) \times 10^{11}$ (m² s⁻¹)そして12-15 MeVで $(1.51 \pm 0.16) \times 10^{10}$ (m² s⁻¹)であった。推定値の誤差には使用した反応断面積の誤差によるものは含まれていない。また, フルエンス率は15 MeV以上のX線フルエンス率が無視できると仮定して推定した。10 MeV以上のエネルギーのX線の量は治療部位へのX線量にほとんど影響を与えない程度であった。しかし, それら高エネルギーのX線はライナックを構成する物質において多くの種類の光核反応を引き起こす。我々のこれまでの研究で照射室内における大きな熱中性子フルエンスが測定されている。10MeVを越えるエネルギーのX線はそれらを生成した光核反応の多くを引き起こしていると推察される。

キーワード: ライナック, 光核反応, 放射線治療, X線